International Journal of Pharmaceutics 416 (2011) 223–228

Contents lists available at ScienceDirect

International Journal of Pharmaceutics

journal homepage: www.elsevier.com/locate/ijpharm

Skin penetration enhancement of core–multishell nanotransporters and invasomes measured by electron paramagnetic resonance spectroscopy

S.F. Haag[a], E. Fleige[b], M. Chen[c], A. Fahr[c], C. Teutloff[d], R. Bittl[d], J. Lademann[e], M. Schäfer-Korting[a], R. Haag[b], M.C. Meinke[e,*]

[a] Freie Universität Berlin, Institut für Pharmazie, Berlin, Germany
[b] Freie Universität Berlin, Institut für Chemie und Biochemie, Berlin, Germany
[c] Friedrich Schiller Universität Jena, Institut für Pharmazie, Pharmazeutische Technologie, Jena, Germany
[d] Freie Universität Berlin, Fachbereich Physik, Berlin, Germany
[e] Charité - Universitätsmedizin Berlin, Department of Dermatology Center of Experimental and Applied Cutaneous Physiology, Charitéplatz 1, 10117 Berlin, Germany

ARTICLE INFO

Article history:
Received 19 April 2011
Accepted 25 June 2011
Available online 1 July 2011

Keywords:
Nanocarriers
Ultra-flexible vesicles
Tape stripping
Multi-frequency EPR

ABSTRACT

In order to cross the skin barrier several techniques and carrier systems were developed to increase skin penetration of topical dermatics and to reduce systemic adverse effects by avoiding systemic application. Ultra-flexible vesicles, e.g. invasomes and core–multishell (CMS) nanotransporters are efficient drug delivery systems for dermatological applications. Electron paramagnetic resonance (EPR) spectroscopic techniques were used for the determination of localization and distribution of the spin label 3-carboxy-2,2,5,5-tetramethyl-1-pyrrolidinyloxy (PCA; log $P = -1.7$) within the carrier systems and the ability of the carriers to promote penetration of PCA into the skin. The results show an exclusive localization of PCA in the hydrophilic compartments of the invasome dispersion and the CMS nanotransporter solution. PCA penetration was enhanced 2.5 fold for CMS and 1.9 fold for invasomes compared to PCA solution. Investigation of penetration depth by step-wise removal of the stratum corneum by tape stripping revealed deepest PCA penetration for invasomes. UV-irradiation of PCA-exposed skin samples revealed that the spin label is still reactive. In conclusion novel polymer-based CMS nanotransporters and invasomes can favor the penetration of PCA or hydrophilic drugs. This offers possibilities for e.g. improved photodynamic therapy.

1. Introduction

In order to cross the stratum corneum of the skin, the main obstacle for the local therapy of skin diseases by the majority of drugs, several techniques and carrier systems were developed. Invasomes (Dragicevic-Curic et al., 2008, 2009) and core–multishell (CMS) nanotransporters (Radowski et al., 2007; Küchler et al., 2009a,b) were shown to be efficient drug delivery systems for hydrophilic and lipophilic agents. Invasomes belong to the group of ultra-flexible liposomal vesicles consisting of phosphatidylcholine, ethanol and terpenes and their liquid membrane allows a better skin penetration of drugs compared to rigid gel state liposomes (El Maghraby et al., 2001). Dragicevic-Curic et al. (2008) have shown a 2-fold enhanced penetration of the photosensitizer temoporfin (mTHPC) into the skin when applied by an invasome dispersion compared to an ethanolic solution and the invasomes appear to deliver sufficient amounts of mTHPC to the skin for topical photodynamic therapy (PDT) of cutaneous malignant (basal-cell carcinoma) or non-malignant diseases (psoriasis). mTHPC penetration efficiency into the skin is low due to its high molecular weight (MW) of 681 g mol^{-1} and unfavorable log P (octanol-water partition coefficient) of 9.2 (Chen et al., 2011). Skin penetration of drugs is best with log P 1–3 and a MW < 500 g mol^{-1} (Korting and Schäfer-Korting, 2010).

Besides skin penetration enhancement, CMS nanotransporters were used for tumor targeting (Quadir et al., 2008), cellular copper uptake by yeast cells (Treiber et al., 2009) or as stabilizers for catalytic platinum nanoparticles (Keilitz et al., 2010). CMS nanotransporters consist of a small polyglycerole core which is surrounded by a lipophilic inner shell and a hydrophilic outer shell. This unit (unimer) has a typical size of 3–5 nm and forms larger aggregates. Küchler et al. (2009a) found a twofold increased penetration of the hydrophilic dye rhodamin B (log $P < 1$) into the stratum corneum and viable epidermis when applied in CMS nanotransporters compared to the application of rhodamin B in a base cream.

Taken together, invasomes and CMS nanotransporters can enhance skin penetration, yet, the question arises which system is most efficient?

* Corresponding author. Tel.: +49 30 450 518 244; fax: +49 30 450 518 918.
E-mail address: martina.meinke@charite.de (M.C. Meinke).

0378-5173/$ – see front matter © 2011 Elsevier B.V. All rights reserved.
doi:10.1016/j.ijpharm.2011.06.044

The evaluation of penetration efficiency by fluorescent dye application is a validated but time consuming method based on cryo sectioning followed by microscopy and picture analysis (Küchler et al., 2009a,b). Tape stripping of the stratum corneum and subsequent determination of the amount of penetrated agent removed is a further method to evaluate penetration efficiency (Meinke et al., 2009). The use of electron paramagnetic resonance (EPR) spectroscopy and application of stable spin labels, e.g. nitroxides, may be a fast alternative for the estimation of penetration efficiency (Sentjurc et al., 1999, 2004; Honzak et al., 2000; Küchler et al., 2010) especially since even the evaluation of quantitative penetration efficiency becomes feasible. Stable spin labels remain active after penetration into the skin and delivered in sufficient amounts, the spin label allows further investigations, e.g. the detection of oxidative stress and free radicals induced by external noxious agents and effects like UV-irradiation (Herrling et al., 2003; Haag et al., 2010) or infrared irradiation (Zastrow et al., 2009; Darvin et al., 2010; Meinke et al., 2010). In fact, the latter may be used to investigate PDT analogue agents.

In order to gain insights into the localization and the microenvironment of the spin label, EPR measurements can reveal the polarity of the immediate surrounding of the spin label as well as the mobility of the label in solution (Smirnov et al., 1995; Lurie and Mäder, 2005; Kempe et al., 2010). We investigated the distribution of the nitroxide spin label PCA (3-carboxy-2,2,5,5-tetramethyl-1-pyrrolidinyloxy; MW = 186 g mol^{-1}; log P = −1.7) (Sano et al., 2000) within an invasome dispersion and CMS nanotransporter solution using high frequency W-band EPR spectroscopy. PCA was selected because it reacts slowly with the skin antioxidant system which is a good prerequisite for the intended comparative penetration measurements (Herrling et al., 2003; Haag et al., 2010). Furthermore, the inherent poor skin penetration due to the low log P value and rather high molecular weight makes PCA an excellent candidate to challenge new carrier systems. Penetration kinetics, efficiency and profile of the PCA from the two formulations were compared to PCA solution using porcine ear skin and low frequency L-band EPR spectroscopy. To our best knowledge, the penetration efficiency of ultra-flexible vesicles and CMS nanotransporters has not yet been compared. Moreover, we studied whether the label is still reactive after penetration into the skin using UV-irradiation.

2. Materials and methods

2.1. Invasome preparation

Invasomes were prepared by mechanical dispersion. Briefly, 5% (w/v) soybean phosphatidylcholine (PC) in ethanol (77.3% PC, 5% lysophosphatidylcholine, 3% cephaline, 1.1% phosphatidic acid of the dry residue and 13.6% ethanol; NAT 8539, Phospholipid, Cologne, Germany) was diluted in a chloroform methanol (2:1) mixture. Organic solvent was removed by rotary evaporation above the lipid transition temperature of 43 °C. Deposited lipid film was hydrated with a mixture of phosphate buffer (pH 7.4; PBS) containing 10% (v:v) ethanol, 1% (w:v) terpenes (limonene:citral:cineole, 1:4.5:4.5, v/v; Sigma–Aldrich, Steinheim, Germany) and 10 mmol l^{-1} 3-carboxy-2,2,5,5-tetramethyl-1-pyrrolidinyloxy (PCA, Sigma–Aldrich, Steinheim, Germany) at room temperature. Resulting vesicles were allowed to swell for 0.5 h, then the suspension was sonicated for 5 min and extruded 21 times through a 100 nm pore membrane at room temperature. Invasomes had a mean particle size of 190 nm with a polydispersity index (PDI) of 0.193 measured by photon correlation spectroscopy (PCS; Zetasizer Nano series, Malvern Instruments, UK).

Table 1
Parameter settings for W- and L-band EPR spectroscopy.

	W-band	L-band
Frequency/GHz	94	1.3
Central magnetic field, B_0/mT	3349	46
Magnetic field sweep width/mT	15	8
Modulation amplitude/mT	0.05	0.15
Lock-in time constant/ms	41	10
Microwave power/mW	0.05	10

2.2. CMS nanotransporter preparation

The CMS nanotransporters with the empirical formula $hPG_{10\,kDa}(-NH_2)_{0.7}(C18mPEG350)_{1.0}$ were prepared by the following procedure (Radowski et al., 2007). Briefly, an excess of 1,18-octadecandioic acid (C18) reacts with monomethyl poly(ethylene glycol) (M_n = 350, mPEG350) in toluene with para-toluenesulfonic acid under Dean-Stark conditions to yield mPEG350-18-oxooctadecanoic acid which was purified by column chromatography. This product was dissolved in methanol and via N-hydroxysuccinimide activation of the acid and reaction with hyperbranched polyglycerolamine (M_n = 10 kDa, degree of amination = 70%, $hPG_{10\,kDa}(-NH_2)_{0.7}$) (Roller et al., 2005) the CMS nanotransporter was formed and purified by subsequent dialysis in methanol (molecular weight cut-off 1000 Da). CMS nanotransporters were dissolved in a small amount of water and lyophilized in order to remove any remaining traces of methanol. For PCA loading lyophilized CMS transporters were dissolved in PBS containing 10% (v:v) ethanol resulting in a 5% (w/v) CMS nanotransporter solution. 10 mmol l^{-1} PCA was added and stirred vigorously for 72 h. Finally the solution was filtrated in order to remove any undissolved impurities. All chemicals, reagents and solvents were of analytical grade and obtained from standard suppliers.

PCS measurements of size distribution by volume revealed 99% for 5 nm unimers and small amounts (<1%) for aggregates 43 nm and 253 nm in size.

2.3. EPR spectroscopy

For the investigation of the label position within the nanocarriers high frequency W-band EPR was performed whereas skin penetration was measured using L-band EPR spectroscopy. EPR spectra were recorded at ambient temperature (22 °C) with parameter settings as summarized in Table 1.

2.4. High frequency W-band measurements

W-band (94 GHz) cw-EPR spectra were recorded on an Elexsys E680 spectrometer with a Teraflex EN600-1021H probehead (Bruker Biospin, Karlsruhe, Germany). PCA formulations were diluted with PBS/10% ethanol to a concentration of 2 mM in order to avoid line broadening. The samples were measured in quartz samples tubes with 0.9 mm outer diameter and 0.3 mm inner diameter (Vitrocom, Mountain Lakes, NJ, USA). Magnetic parameters were determined using the EasySpin toolbox (Stoll and Schweiger, 2006). The information content of EPR spectra varies with the employed microwave frequency. The higher the frequency in EPR spectroscopy the sensitivity increases and the more information about the microenvironment of a spin label can be obtained. 94 GHz W-band measurements can reveal the polarity of the immediate surrounding of a spin label as well as its rotational correlation time (mobility of the label) in aqueous carrier solutions (Smirnov et al., 1995) and, therefore, give information about the localization of the label (Braem et al., 2007).

2.5. Low frequency L-band measurements

L-band (1.3 GHz) cw-EPR spectra were recorded on a LBM MT 03 spectrometer with a surface coil type resonator (Magnettech, Berlin, Germany). At L-band frequencies measurements of aqueous solutions, nanomaterial of up to 1 ml and skin biopsies become feasible (W-band sample volume is only 1 μl). Liquids were analyzed in 1.5 ml reaction tubes (Eppendorf AG, Hamburg, Germany). For skin (full thickness) penetration measurements the tissue fixed on microscopic slides using cyanoacrylate glue (Uhu, Bühl, Germany) was positioned exactly using a micrometer screw. For all experiments the signal intensity was calculated by a double integration of the spectra (Analysis 3.3 software, Magnettech, Berlin, Germany).

2.6. Skin penetration studies

For the skin penetration studies porcine ear skin was used, as it is a suitable model for human skin (Meyer et al., 1978; Haag et al., 2010). The ears were delivered from a local butcher with approval by the Veterinary Office Berlin-Treptow on the day of slaughter, washed thoroughly and dried with paper towels. Hairs were completely removed by clipping, taking care to avoid skin injury. Punch biopsies 19 mm in diameter, approximately 1.5 mm of full thickness skin were taken in the centre of the ear and fixed onto microscopic glass slides.

Before entering into the comparison of carrier related skin penetration we had to prove that PCA degradation by the skin antioxidant system does not depend on the vehicle constituents of the formulation to ensure equal penetration conditions. Therefore, the decline of PCA intensity during penetration into porcine ear skin was investigated following the application of PCA (10 mmol l^{-1}, 10 μl cm^{-2}) invasomes, CMS nanotransporters and solution, respectively. A silicon barrier was used in order to avoid lateral spreading and the test material was evenly spread on the skin surface. The skin samples with the applied test materials were immediately subjected to L-band EPR measurements which were subsequently repeated every 4 min up to 30 min and the signal intensity of PCA on the skin surface as well as of penetrated PCA was recorded.

Then PCA penetration was studied. Skin samples (prepared as described above) exposed to the formulations of the spin label (10 mmol l^{-1}, 20 μl cm^{-2}) for 30 min. The remaining material was removed from the skin surface using paper towels and the treated areas were subjected to L-band EPR spectroscopy (baseline data). Afterwards the samples were irradiated with UV light for 1 min (280–400 nm; TH-1E; Cosmedico Medizintechnik, Villingen-Schwenningen, Germany) in order to test whether the label PCA is still reactive and recombines with short-living free radicals. Irradiation intensity was 3.8 mW cm^{-2} measured by the power meter HBM-1 (Hydrosun Medizintechnik, Mülheim, Germany).

For approximation of relative penetration depth of the spin label the tape stripping technique was used (Jacobi et al., 2005). 30 min after application of the formulations and removal of surplus material, up to 7 tape strips (Tesa Film, Beiersdorf, Hamburg, Germany) were taken from treated skin samples which were immediately subjected to the L-band EPR spectrometer before and after each strip taken.

2.7. Statistical analysis

Arithmetical mean values and standard errors of mean (SEM) of the data are reported. For explorative data analysis, the program PASW for Windows (SPSS, Chicago, IL, USA) was used. First, with the related samples Friedman's two way analysis of variances by ranks was performed. Differences among the means of groups were analyzed by the Wilcoxon test, considering significance at $p \leq 0.05$, and a trend at $p \leq 0.1$.

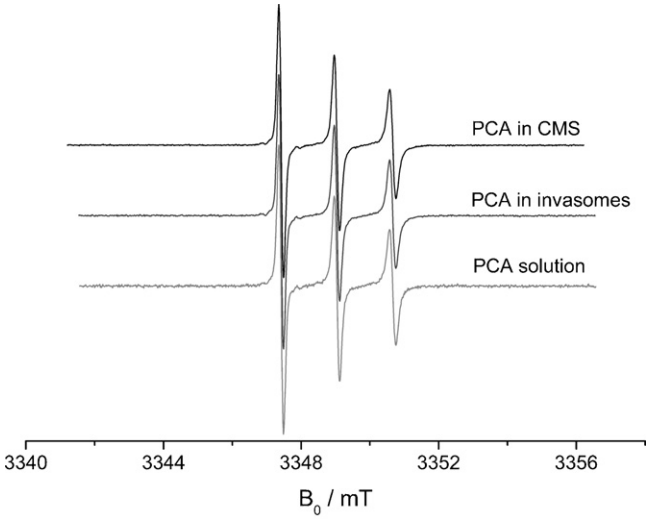

Fig. 1. EPR spectra of PCA containing CMS, invasomes and PCA in solution. Measurements were performed at W-band frequency (94 GHz) at room temperature. For better visualization an offset was added to the spectra. The results show an equal polarity and a comparable mobility of PCA containing carriers and PCA in solution.

3. Results

3.1. High frequency W-band analysis

Microenvironment investigation of the label was performed using high-frequency W-band measurements at room temperature (Fig. 1). *g*-Value (g_{iso} = 2.0054), hyperfine coupling constant (A_{iso} = 46 MHz) and rotational correlation time (6×10^{-11} s) were found to be the same for the three formulations. The *g* and A_{iso} value show an equal polarity of the label within the formulations and the label can be located in both, interior and exterior aqueous phases of the carrier. The rotational correlation time of PCA indicates an equal mobility sensed by the label within the systems. For spectral simulation following parameters for the *g*-value: g_{xx} = 2.0089, g_{yy} = 2.0060, g_{zz} = 2.0012 and for the hyperfine coupling: A_{xx} = 30 MHz, A_{yy} = 35 MHz, A_{zz} = 72 MHz were used. Dilution assays of invasomes, too, have shown an equal PCA distribution between inside and outside which is due to the fact that PCA is capable of membrane crossing (data not shown).

3.2. Skin penetration efficiency

The reaction of PCA with the skin antioxidant system was not influenced by the vehicle compounds of the formulations. The decline of the intensity of the spin label signal after a 30 min penetration time into porcine skin was 21% for PCA invasomes, 20% for CMS nanotransporters and 18% when applying the solution (data not shown). Therefore, the inherent PCA degradation within the skin is independent of the formulation.

Fig. 2 shows the signal intensities of the skin following the application of the test formulations 30 min to porcine skin and removal of the surplus formulation from the skin surface. Compared to the solution PCA penetration was enhanced by 1.9- and 2.5-fold when applied within invasomes and CMS nanotransporters, respectively, and penetration enhancement by CMS nanotransporters was 1.3-fold compared to the uptake from invasomes. Statistical analysis revealed significant ($p < 0.05$) penetration enhancement by both nanocarriers compared to PCA solution. The differences between CMS nanotransporters and invasomes showed a trend

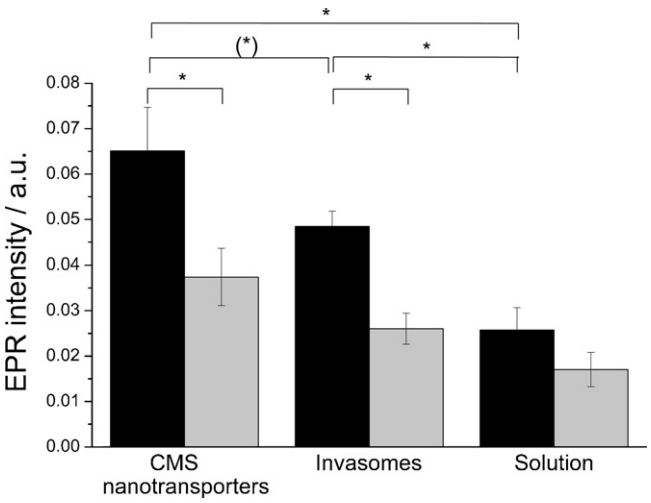

Fig. 2. Mean EPR intensity ± SEM of PCA treated skin after a 30 min penetration time and removal of remaining liquid from the skin surface (black column) as well as PCA reactivity to UV-induced free radicals (grey column). $*p < 0.05$, $(*)p < 0.1$, $(n = 6)$.

($p = 0.07$) for the superior efficiency of the former. Furthermore, after subsequent UV-irradiation PCA still reacts to short-living free radicals when applying PCA within invasomes and CMS nanotransporters. The mean values before and after UV-irradiation show significant differences ($p < 0.05$) for CMS nanotransporters and for invasomes but not for PCA solution. Both nanocarriers deliver sufficient amounts of the spin label into the skin for oxidative stress measurements.

Fig. 3 presents the results from the tape stripping experiments, which are in accordance with the penetration efficiency depicted in Fig. 2. Following the application of CMS nanotransporters PCA penetration was particularly high in unstripped skin and declined exponentially as to be derived from the decline of signal intensity of the skin with subsequently taken tape strips. In fact, after one strip the intensity declines to only 25% and an EPR signal is no longer detected after tape 6. In contrast following the invasomes, PCA signal intensity declines less steeply and EPR signal is still detectable with tape 6. Applying PCA solution, the spin label penetrates the skin only poorly. Signal is low from start on and after tape 4 below the detection limit.

4. Discussion

Stimulated by the various options for skin penetration enhancement which becomes possible by various drug carrier systems (Korting and Schäfer-Korting, 2010) we compared two nanocarriers which appear to be particularly efficient, invasomes and CMS nanotransporters, using a spin label as model agent.

The results derived from high frequency W-band measurements of both carriers indicate an equal microenvironment (polarity and mobility) of the nitroxide PCA as it was observed in a solution of PBS with 10% ethanol (Fig. 1), which served for reference. No partitioning of the label into the lipid membrane of the invasome and into the lipophilic polymers of the CMS nanotransporters could be derived from the recorded spectra. This is probably due to the hydrophilic properties of PCA, consisting of a pyrrolidine ring with a carboxyl group ($\log P = -1.7$). For invasomes the label can be located in both, the outside and the inside buffer regions of the vehicle, as confirmed by dilution measurements. For CMS nanotransporters the results indicate that PCA can be located in the hydrophilic CMS matrix as well as in the buffer. Braem et al. (2007) loaded spin labels on the surface of solid lipid nanoparticles and found that the spin labels were attached in two distinct sub-compartments: the rim and the flat surface of the disk-like shapes. This could be determined by EPR spectroscopy since the spin labels exhibit different rotational correlation times (mobility) depending on the sub-compartment they are attached to. This was not found for the spin label PCA used in the nanocarriers in this study although at 94 GHz even small changes in the rotational correlation time affect the spectrum significantly as can be demonstrated by simulations (Stoll and Schweiger, 2006).

4.1. Skin penetration measurements

The change of EPR intensity during penetration into porcine ear skin revealed a PCA intensity decline after 30 min for all three formulations by about 20%. This can be due to the interaction of the semi stable free radical PCA with the skin antioxidant system that causes a reduction of PCA to the EPR-silent hydroxylamine. This inactivation occurs on as well as inside the skin. The antioxidant system of the skin consists of enzymatic and non-enzymatic reducing agents, in particular the thioredoxin/thioredoxin reductase system, glutathione, ascorbic acid and vitamin E (Schallreuter and Wood, 1986, 2001; Thiele et al., 1998, 2001). Lateral spreading of the spin label out of the measurement volume was prevented by

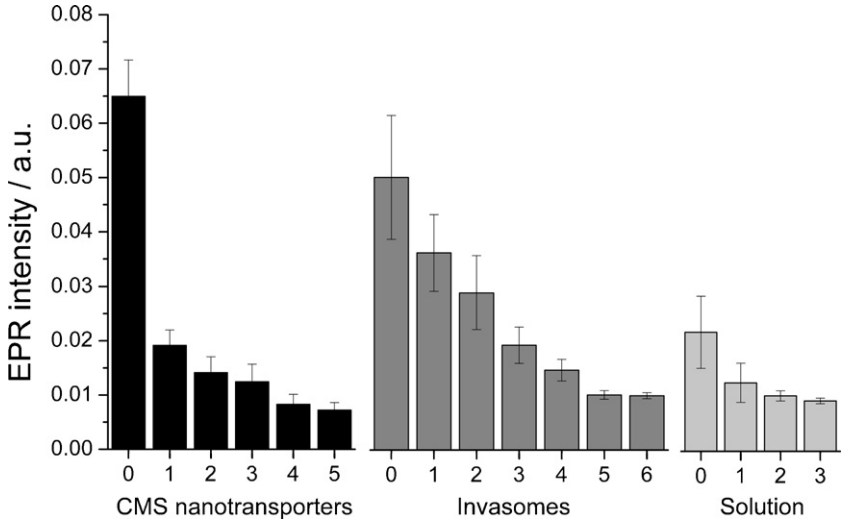

Fig. 3. Spin label intensity of tape stripped porcine skin 30 min after application of PCA formulations. Tape number 0 corresponds to the intensity after penetration and removal of remaining liquids, number 1–6 correspond to the PCA related signal intensity of the skin after each tape strip taken. Mean ± SEM ($n = 3$).

a homogeneous distribution of the test material on the skin surface and an additional silicon barrier.

Depending on the polarity of the loaded drug, its interaction with the carrier and its distribution profiles within the carrier matrix, different release patterns can be expected. In contrast to the hydrophilic label PCA ultra flexible vesicles (e.g. invasomes) with a membrane located lipophilic spin label would result in stabilization and prolonged release of the label whereas application in solution would result in a burst release as it was shown for the drug pergolide (Honeywell-Nguyen and Bouwstra, 2003). The stabilizing effect of invasomes has recently been shown for the amphiphilic spin label 2,2,6,6-tetramethyl-1-piperidinyloxy (Haag et al., 2011). One explanation for the comparable PCA intensity decline could be the fast disintegration of small, ultra flexible invasomes (Sentjurc et al., 1999) after skin exposure and the localization of PCA in the accessible hydrophilic regions of the CMS nanotransporters. Therefore, PCA interaction with the skin when applied with nanocarriers appears to be comparable to the application of PCA solution. Yet, the rather close decrease for all three formulations is a good prerequisite for comparative penetration studies.

The investigation of penetration efficiency revealed a significantly better penetration of PCA from CMS nanotransporters (2.5-fold) and invasomes (1.9-fold) compared to PCA solution (Fig. 2). PCA penetration enhancement when applying invasomes is well in accordance with a twofold increase of the photosensitizer mTHPC penetration when comparing invasomes to an ethanolic solution (Dragicevic-Curic et al., 2008). Moreover also the penetration of the hydrophilic dye rhodamin B into the stratum corneum and epidermis of porcine skin was enhanced twofold compared to a base cream by rhodamin B loading to CMS nanotransporters (Küchler et al., 2009a) and compared to PCA penetration the results are rather close. In fact, this underlines the enhanced penetration of CMS nanotransporters when aiming to apply a hydrophilic agent to the skin.

The efficient penetration of PCA when applied in CMS nanotransporters can be explained by the size of the carrier. While invasomes had a mean size of 190 nm, the CMS nanotransporters exhibited a mean size of 5 nm only and thus may penetrate the less dense superficial horny layer (Korting and Schäfer-Korting, 2010). Well in accordance with the hypothesis is the strong intensity decline of PCA related signal already after the first tape strip (Fig. 3), which indicates that CMS nanotransporters penetrate mainly the very superficial stratum corneum. In contrast to CMS nanotransporters the invasome membrane or membrane constituents can disintegrate the stratum corneum forming channel-like pathways through which drug molecules penetrate (van den Bergh et al., 1999) resulting in a deeper penetration of PCA when applied by invasomes. For the total PCA amount measured integrally the disintegration mechanism of invasomes could be less effective than direct penetration of small CMS nanotransporters. On the other hand up to tape 6 PCA was well quantified in the skin when applied with invasomes. The rather linear decrease indicates most efficient invasion of the skin by the carrier system.

To gain even more detailed insights in the penetration enhancing mechanisms of nanocarriers the use of lipophilic or amphiphilic spin labels might be helpful since these compounds partition in environments differing in polarity which is detectable by EPR spectroscopy.

Regarding UV-irradiation of PCA-containing skin samples the spin label still reacts with UV-induced short living free radicals regardless which formulation was applied. Nevertheless, due to the PCA penetration enhancement by CMS nanotransporters and invasomes the mean values before and after UV-irradiation differ significantly, whereas the amount of PCA in the skin was too low after application of PCA solution to achieve a significant decline after UV-irradiation. For the evaluation of carriers to deliver sufficient amounts of photosensitizer for PDT, the use of PCA or spin labeled photosensitizer and subsequent UV-irradiation appears promising.

In conclusion, both polymer based CMS nanotransporters and lipid based invasomes were shown to be efficient drug delivery systems for topical application of hydrophilic substances to the skin. Nevertheless, the direct comparison has shown a trend to higher penetration enhancement for CMS nanotransporters in the upper layers of the stratum corneum whereas the invasomes appear to deliver agents in particular to deeper stratum corneum layers. EPR based detection and estimation of penetration efficiency is a fast alternative to fluorescence dye techniques as the results obtained are comparable. Especially the hydrophilic spin label PCA was found suitable for comparison of the efficiency of nanocarrier systems. Yet it has to be kept in mind that compared to EPR fluorescence techniques allow the detection of the dye in the viable epidermis and dermis, too. EPR based investigations, however, can reveal additional information about the localization of the label within the carrier formulation and its microenvironment.

Acknowledgment

This work was funded by the Freie Universität Berlin, Focus Area Functional Nanoscale Materials.

References

Braem, C., Blaschke, T., Panek-Minkin, G., Herrmann, W., Schlupp, P., Paepenmüller, T., Müller-Goyman, C., Mehnert, W., Bittl, R., Schäfer-Korting, M., Kramer, K.D., 2007. Interaction of drug molecules with carrier systems as studied by parelectric spectroscopy and electron spin resonance. J. Control. Release 119, 128–135.

Chen, M., Liu, X., Fahr, A., 2011. Skin penetration and deposition of carboxyfluorescein and temoporfin from different lipid vesicular systems: in vitro study with finite and infinite dosage application. Int. J. Pharm., doi:10.1016/j.ijpharm.2011.02.006.

Darvin, M.E., Haag, S.F., Lademann, J., Zastrow, L., Sterry, W., Meinke, M.C., 2010. Formation of free radicals in human skin during irradiation with infrared light. J. Invest. Dermatol. 130, 629–631.

Dragicevic-Curic, N., Scheglmann, D., Albrecht, V., Fahr, A., 2008. Temoporfin-loaded invasomes: development, characterization and in vitro skin penetration studies. J. Control. Release 127, 59–69.

Dragicevic-Curic, N., Scheglmann, D., Albrecht, V., Fahr, A., 2009. Development of different temoporfin-loaded invasomes-novel nanocarriers of temoporfin: characterization, stability and in vitro skin penetration studies. Colloids Surf. B: Biointerfaces 70, 198–206.

El Maghraby, G.M., Williams, A.C., Barry, B.W., 2001. Skin delivery of 5-fluorouracil from ultradeformable and standard liposomes in-vitro. J. Pharm. Pharmacol. 53, 1069–1077.

Haag, S.F., Bechtel, A., Darvin, M.E., Klein, F., Groth, N., Schäfer-Korting, M., Bittl, R., Lademann, J., Sterry, W., Meinke, M.C., 2010. Comparative study of carotenoids catalase and radical formation in human and animal skin. Skin Pharmacol. Physiol. 23, 306–312.

Haag, S.F., Chen, M., Taskoparan, B., Fahr, A., Bittl, R., Teutloff, C., Wenzel, R., Lademann, J., Schäfer-Korting, M., Meinke, M.C., 2011. Stabilisation of reactive nitroxides using Invasomes to allow prolonged electron paramagnetic resonance measurements. Skin Pharmacol. Physiol, doi:10.1159/000330235.

Herrling, T., Fuchs, J., Rehberg, J., Groth, N., 2003. UV-induced free radicals in the skin detected by ESR spectroscopy and imaging using nitroxides. Free Radic. Biol. Med. 35, 59–67.

Honeywell-Nguyen, P.L., Bouwstra, J.A., 2003. The in vitro transport of pergolide from surfactant-based elastic vesicles through human skin: a suggested mechanism of action. J. Control. Release 86, 145–156.

Honzak, L., Sentjurc, M., Swartz, H.M., 2000. In vivo EPR of topical delivery of a hydrophilic substance encapsulated in multilamellar liposomes applied to the skin of hairless and normal mice. J. Control. Release 66, 221–228.

Jacobi, U., Weigmann, H.J., Ulrich, J., Sterry, W., Lademann, J., 2005. Estimation of the relative stratum corneum amount removed by tape stripping. Skin Res. Technol. 11, 91–96.

Keilitz, J., Schwarze, M., Nowag, S., Schomacker, R., Haag, R., 2010. Homogeneous stabilization of Pt nanoparticles in dendritic core–multishell architectures: application in catalytic hydrogenation reactions and recycling. Chemcatchem 2, 863–870.

Kempe, S., Metz, H., Mäder, K., 2010. Application of electron paramagnetic resonance (EPR) spectroscopy and imaging in drug delivery research—chances and challenges. Eur. J. Pharm. Biopharm. 74, 55–66.

Korting, H.C., Schäfer-Korting, M., 2010. Carriers in the topical treatment of skin disease. Handb. Exp. Pharmacol., 435–468.

Küchler, S., Abdel-Mottaleb, M., Lamprecht, A., Radowski, M.R., Haag, R., Schäfer-Korting, M., 2009a. Influence of nanocarrier type and size on skin delivery of hydrophilic agents. Int. J. Pharm. 377, 169–172.

Küchler, S., Herrmann, W., Panek-Minkin, G., Blaschke, T., Zoschke, C., Kramer, K.D., Bittl, R., Schäfer-Korting, M., 2010. SLN for topical application in skin diseases—characterization of drug-carrier and carrier–target interactions. Int. J. Pharm. 390, 225–233.

Küchler, S., Radowski, M.R., Blaschke, T., Dathe, M., Plendl, J., Haag, R., Schäfer-Korting, M., Kramer, K.D., 2009b. Nanoparticles for skin penetration enhancement—a comparison of a dendritic core–multishell-nanotransporter and solid lipid nanoparticles. Eur. J. Pharm. Biopharm. 71, 243–250.

Lurie, D.J., Mäder, K., 2005. Monitoring drug delivery processes by EPR and related techniques—principles and applications. Adv. Drug Deliv. Rev. 57, 1171–1190.

Meinke, M., Abdollahnia, M., Gahr, F., Platzek, T., Sterry, W., Lademann, J., 2009. Migration and penetration of a fluorescent textile dye into the skin—in vivo versus in vitro methods. Exp. Dermatol. 18, 789–792.

Meinke, M.C., Haag, S.F., Schanzer, S., Groth, N., Gersonde, I., Lademann, J., 2010. Radical protection by sunscreens in the infrared spectral range. Photochem. Photobiol., doi:10.1111/j.1751-1097.2010.00838.x.

Meyer, W., Schwarz, R., Neurand, K., 1978. The skin of domestic mammals as a model for the human skin, with special reference to the domestic pig. Curr. Probl. Dermatol. 7, 39–52.

Quadir, M.A., Radowski, M.R., Kratz, F., Licha, K., Hauff, P., Haag, R., 2008. Dendritic multishell architectures for drug and dye transport. J. Control. Release 132, 289–294.

Radowski, M.R., Shukla, A., von, B.H., Bottcher, C., Pickaert, G., Rehage, H., Haag, R., 2007. Supramolecular aggregates of dendritic multishell architectures as universal nanocarriers. Angew. Chem. Int. Ed. Engl. 46, 1265–1269.

Roller, S., Zhou, H., Haag, R., 2005. High-loading polyglycerol supported reagents for Mitsunobu- and acylation-reactions and other useful polyglycerol derivatives. Mol. Divers. 9, 305–316.

Sano, H., Naruse, M., Matsumoto, K., Oi, T., Utsumi, H., 2000. A new nitroxyl-probe with high retention in the brain and its application for brain imaging. Free Radic. Biol. Med. 28, 959–969.

Schallreuter, K.U., Wood, J.M., 1986. The role of thioredoxin reductase in the reduction of free radicals at the surface of the epidermis. Biochem. Biophys. Res. Commun. 136, 630–637.

Schallreuter, K.U., Wood, J.M., 2001. Thioredoxin reductase—its role in epidermal redox status. J. Photochem. Photobiol. B 64, 179–184.

Sentjurc, M., Kristl, J., Abramovic, Z., 2004. Transport of liposome-entrapped substances into skin as measured by electron paramagnetic resonance oximetry in vivo. Methods Enzymol. 387, 267–287.

Sentjurc, M., Vrhovnik, K., Kristl, J., 1999. Liposomes as a topical delivery system: the role of size on transport studied by the EPR imaging method. J. Control. Release 59, 87–97.

Smirnov, A.I., Smirnova, T.I., Morse, P.D., 1995. Very high frequency electron paramagnetic resonance of 2,2,6,6-tetramethyl-1-piperidinyloxy in 1,2-dipalmitoyl-sn-glycero-3-phosphatidylcholine liposomes: partitioning and molecular dynamics. Biophys. J. 68, 2350–2360.

Stoll, S., Schweiger, A., 2006. EasySpin, a comprehensive software package for spectral simulation and analysis in EPR. J. Magn. Reson. 178, 42–55.

Thiele, J.J., Schroeter, C., Hsieh, S.N., Podda, M., Packer, L., 2001. The antioxidant network of the stratum corneum. Curr. Probl. Dermatol. 29, 26–42.

Thiele, J.J., Traber, M.G., Packer, L., 1998. Depletion of human stratum corneum vitamin E: an early and sensitive in vivo marker of UV induced photo-oxidation. J. Invest. Dermatol. 110, 756–761.

Treiber, C., Quadir, M.A., Voigt, P., Radowski, M., Xu, S., Munter, L.M., Bayer, T.A., Schaefer, M., Haag, R., Multhaup, G., 2009. Cellular copper import by nanocarrier systems, intracellular availability, and effects on amyloid beta peptide secretion. Biochemistry 48, 4273–4284.

van den Bergh, B.A., Bouwstra, J.A., Junginger, H.E., Wertz, P.W., 1999. Elasticity of vesicles affects hairless mouse skin structure and permeability. J. Control. Release 62, 367–379.

Zastrow, L., Groth, N., Klein, F., Kockott, D., Lademann, J., Renneberg, R., Ferrero, L., 2009. The missing link–light-induced (280–1600 nm) free radical formation in human skin. Skin Pharmacol. Physiol. 22, 31–44.